

Original Article

Genetic Algorithm Turned PID Control of AFPMSM for Electrical Vehicle Application

Nguyen Van Hai¹, Vo Thanh Ha²

^{1,2}Faculty of Electrical and Electronic Engineering, University of Transport and Communications, Hanoi, Vietnam.

²Corresponding Author : vothanha.ktd@utc.edu.vn

Received: 23 November 2023

Revised: 16 December 2023

Accepted: 23 January 2024

Published: 16 February 2024

Abstract - This article describes the development of a torque controller for an Axial Flux Permanent Magnet Synchronous Motor (AFPMSM) using a Genetic Algorithm (GA) to optimize the two parameters of the PI controller. The GA aims to select the optimal set of two (K_p , K_i , K_d) for the PID controller, satisfying one of the objective functions IAE, ITAE, and MSE. After offline gene selection, regeneration, and mutation with upper and lower limit conditions, the two parameters of the PI controller are optimized to achieve the required torque and speed responses of the AFPMSM motor. The accuracy of the theory is validated through offline MATLAB/SIMULINK. The use of the genetic algorithm for optimizing the PID controller parameters has proven effective in achieving the desired torque and speed responses of the AFPMSM, demonstrating its potential for practical application in real-world scenarios. The optimized PID controller parameters can significantly improve the performance of the axial flux permanent magnet synchronous motor, leading to more precise torque and speed control. This approach offers a practical and efficient method for achieving desired motor responses, and it has the potential to be applied in various industrial and commercial applications. The use of genetic algorithms in motor control optimization demonstrates the continued advancements in control systems and their ability to meet the demands of real-world scenarios.

Keywords - AFPMSM, GA, PID, Electrical Vehicle, QRF.

1. Introduction

Traction drive systems in different industries, such as transportation (electric cars, buses, marine applications, and civil and industrial machinery), need higher torque density and speed range for electric drive systems [1]. The permanent magnet axial magnetic motor (AFPMSM) is notable for its small size, high torque density, and minimal torque pulsation, making it a preferred choice for traction systems [2]. Research shows that the AFPMSM, which has permanent magnets in the rotor, effectively reduces losses in the magnetic circuit, leading to significantly lower rotor losses and improved performance and power density [3]. Furthermore, studies indicate that the multi-pole structure and axial flux of the AFPMSM require very little core material, achieving a high moment/weight ratio, with the added advantage of reduced noise and vibration compared to traditional AC and DC electric motors [4-6]. The design and manufacturing of AFPMSM with easily adjustable air gaps further enhances its appeal across various applications.

The AFPMSM is optimized for torque and speed control through Direct Torque Control (DTC), Quasi Rotor Flux (QRF), and a combination of control algorithms, both linear (PI, LQR, Dead beat...) and nonlinear (sliding control, flat support, fuzzy logic...) [7, 8]. The research focuses on

assessing these solutions' effectiveness for torque and speed control, especially under dynamic load torque conditions, to minimize torque pulsation and achieve precise speed response [9-12]. Intelligent control solutions are being investigated to improve the torque response of AFPMSM, taking into account the impact of various physical properties of electric cars, such as brake pedal, foot pedal, throttle, road inclination, and wind resistance, to enhance electric vehicle performance and ensure sustainable control of electric car powertrains. However, despite these efforts, there is still a lack of published works in this area. This article outlines the design of a single-sided AFPMSM torque controller (one stator and one rotor) using the PID parameter optimization method with a Genetic Algorithm (GA). The controller aims to attain values (K_{p_opt} , K_{i_opt} , K_{d_opt}) that meet the objective functions within a limited search space. The PI controller is adjusted to the optimal K_p , K_i , and K_d coefficients without needing prior experience or a reference for determining optimal values for parameter fine-tuning [13-16]. The effectiveness of the GA-PID controller will be compared with the PID controller through MATLAB/SIMULINK simulation.

The article consists of five main parts. The first part discusses the necessity of researching to enhance the torque and speed response for AFPMSM applied to electric cars. Part



2 presents the mathematical model of the electric car traction drive system. Part 3 details the mathematical equations for designing the GA_PID controller and demonstrates the theory's accuracy. Part 4 showcases simulation results on current and torque responses between the GA_PID and traditional PID controller. Finally, the article concludes by highlighting the contributions of the research and suggesting future directions to improve and enhance torque response and sustainability of traction transmission systems in both theory and experimental implementation.

2. AFPMSM Mathematical Model and Load

2.1. Mathematical Model AFPMSM

The 1-sided AFPMSM means that the AFPMSM motor has one stator and one rotor. Therefore, the AFPMSM can use the Permanent Magnet Synchronous Motor (PMSM) model [12]. However, the AFPMSM mathematical model has differences in stator winding parameter values, and the motor Back-EMF generated by a permanent magnet and an excitation coil does not differ. The stator voltage equation in the d-q reference system is calculated according to Equations (1), and (2).

The application method is written as follows:

$$\begin{bmatrix} u_{sd} \\ u_{sq} \end{bmatrix} = \begin{bmatrix} R_{sq} + \frac{dL_{sq}}{dt} & \omega_m L_{sd} \\ -\omega_m L_{sd} & R_{sd} + \frac{dL_{sd}}{dt} \end{bmatrix} \begin{bmatrix} i_{sd} \\ i_{sq} \end{bmatrix} + \begin{bmatrix} \omega_m \lambda_m \\ 0 \end{bmatrix} \quad (1)$$

The moment equation is determined as follows:

$$T_m = \frac{3P}{2} (L_{sd} i_{sd} + \lambda_m) i_{sq} - (L_{sq} i_{sq}) \quad (2)$$

Since the information is a constant, the proportional description is convenient for the flow stator axis of rotation q. The Equation selects the electromagnetic module submission (3):

$$T_m = \frac{3}{4} P \lambda_m i_{sq} \quad (3)$$

2.2. Mathematica Model of Electric Cars

Drive wheel model as formula (4):

$$\begin{cases} v_{Wh} = \omega_{Wh} R_{Wh} \\ T_{Wh} = T_L = F_r R_{Wh} \end{cases} \quad (4)$$

When the wheel presses against the road surface with force N and is driven by a torque of T_{wh}, The vehicle will exert a force on the road surface F; Correspondingly, the road surface acts against the vehicle with a force of the same value in the opposite direction Ft.

In this case, then Ft is the force of friction and is the useful force component that creates the movement of the vehicle at speed V_x

$$F_t = m_v \cdot g \cdot \mu \quad (5)$$

Applying Newton's second law to the external force components acting on the vehicle body, we have the Equation (6):

$$m_v \frac{dv_{ev}}{dt} = F_t - F_{aero} - F_{roll} - m_v \cdot g \cdot \sin(\alpha) \quad (6)$$

2.2.1. Air Resistance

$$F_{aero} = \frac{\rho C_d A_F}{2} (v_{ev} + v_{wind})^2 \quad (7)$$

In some cases or simulations, we can consider wind speed v_{wind} = 0 . Rolling resistance exists in case the tire is under-inflated:

$$F_{roll} = f_r F_{zY} \quad (8)$$

$$F_{zY} = m_v g \cos(\alpha) \quad (9)$$

3. Design of Torque Controller

3.1. Design of PID Torque Controller

The design of torque controllers for the AFPMSM motor becomes essential in high-performance applications. The design procedure for synthesizing and implementing current controllers for the AFPMSM is similar to current controllers for asynchronous motor drives. To design a torque controller for AFPMSM, it is necessary to clearly understand the interaction of the motor, inverter, and current controller. Therefore, assume the gain of the inverter is K_r and the time constant of the inverter is T_r, which is half the period of the Pulse Width Modulation (PWM) carrier frequency. Besides, if the desired performance of the current control loop is the same as the system is a first-order hysteresis.

$$\frac{i_d}{i_d^*} = \frac{K_i}{1 + sT_i} \quad (10)$$

3.1.1. Current Loop

$$\frac{i_q}{i_q^*} = \frac{K_a K_i (1 + T_m s)}{H_c K_a K_r (1 + sT_m) + (1 + sT_r) \{K_a K_b + (1 + sT_a)(1 + sT_m)\}} \quad (11)$$

The following approximations are valid near the vicinity of the crossover frequency.

$$(1 + sT_a)(1 + sT_r) \cong 1 + s(T_a + T_r) \cong 1 + sT_{ar} \quad (12)$$

The current transfer function is rewritten as follows:

$$\frac{i_q}{i_q^*} = \frac{(K_a K_i T_m) s}{K_a K_b + (T_m + K_a K_i T_m H_c) s + (T_m T_{af}) s^2}$$

$$\frac{n!}{r!(n-r)!} \cong \left(\frac{K_r T_m}{K_b} \right) \frac{s}{(1+sT_1)(1+sT_2)} \quad (13)$$

Where, $T_1 < T_2 < T_m$ and based on further estimates, $(1+sT_2) \cong sT_2$ then the transfer function of the current loop is given by:

$$\frac{i_q}{i_q^*} \cong \frac{K_i}{(1+sT_i)} \quad (14)$$

Where, $K_i = \frac{T_m K_r}{T_2 K_b}$; $T_i = T_1$

3.2. Design of GA_PID Torque Controller

First, the control object is considered a black box suitable for real applications. A behavioral identification cycle of the system is established based on the open-loop step response of the object. From this response, the Genetic Algorithm (GA) is applied to determine three parameters of the PID controller. These three parameters are the basis for limiting the search space of the Genetic Algorithm.

The task of the Genetic Algorithm is to select the two sets {Kp, Ki, Kd} optimal for the PID controller, satisfying one of the objective functions IAE, ITAE, and MSE. These objective functions will calculate the difference between the set value and the actual value, so the objective functions of the controller adjustment process in this problem are defined as follows:

IAE (Integral of Absolute Error):

$$J_1 = \int_0^{\infty} |e(t)| dt: \text{Absolute error integration}$$

IATE (Integral of Time and Absolute Error):

$$J_3 = \int_0^{\infty} t |e(t)| dt: \text{Integral of time and absolute error.}$$

MSE (Mean Squared Error):

$$J_4 = \frac{1}{N} \sum_0^{\infty} |e(t)|^2 dt: \text{squared error}$$

The Genetic Algorithm will be based on three sets of parameters of the PID controller and use the above three objective functions to calculate the error between the set and actual values.

Based on the results, it is found that the objective function with the largest value will be selected to select the third set {Kp, Ki, Kd} optimized for PID controllers. The task of the applied GA algorithm is to find values {Kp_opt, Ki_opt, Kd_opt} optimization of the PID controller, for which the

objective functions of the Genetic Algorithm are: $\min \{J_i (i=1,2,3)\}$. In order to limit the search space of the Genetic Algorithm, we assume optimal values {Kp_opt, Ki_opt, Kd_opt} lie around the value {Kp_Z_N, Ki_Z_N} achieved from the Genetic Algorithm. The corresponding search limits for the two parameters of the PID controller are as follows:

$$\alpha Kp_Z_N \leq Kp_opt \leq \beta Kp_Z_N \quad (15)$$

$$\alpha Ki_Z_N \leq Ki_opt \leq \beta Ki_Z_N \quad (16)$$

$$\alpha Kd_Z_N \leq Kd_opt \leq \beta Kd_Z_N \quad (17)$$

Where coefficients α and β are chosen so that the search space is large enough to contain the desired optimal value, simulation results on the engine speed control system model show $\alpha=0,02$ and $\beta=50$ are satisfying.

The Genetic Algorithm is supported by MATLAB software and is presented in detail in the MathWorks Inc., 2020. In this context, the GA tool in MATLAB is introduced and is only used as a tool to solve optimization problems in order to achieve the following values.

{Kp_opt, Ki_opt, and Kd_opt} satisfy the objective functions with the search space limited by (19) & (20). The parameters of the Genetic Algorithm in this study are selected as follows: evolutionary processive r 100 generations (generations = 100); population size 100 (population size = 100); hybridization frequency 0,8 (Crossover Fraction = 0,8); The mutation probability is adaptively adjusted in the range from 0,001 from 0,01, upper limit $ub = [0 \ 0]$, lower border $ub = [50 \ 50]$, The search space is three elements Kp to Ki to Kd. The optimization time of three PID parameters with max chromosome is 100.

4. Simulation Results and Evaluation

4.1. Build Operating Modes for Electric Car

The operating mode of electric cars is built as follows:

- Initially, the car is stationary, velocity $v = 0$, and the accelerator and brake pedal do not act.
- When the accelerator pedal impacts, the vehicle begins to accelerate, velocity $v > 0$ cubes, comparing state transition conditions. The torque set Te^* is determined by adding the output value of the interpolation table between the accelerator and brake pedals.

The traction drive system control structure for electric cars using AFPMSM motors integrates wheels, as shown in Figure 1.

To evaluate the controller efficiency for traction drive systems for electric vehicles using wheel-integrated AFPMSM motors, the system was simulated on MATLAB with the following simulation scenario:

- Assumes an acceleration of wind speed of zero.
- The car moves on a flat road, but at the time of $t = 3.5s$ to $4.3s$, the vehicle goes downhill.
- At time $t = 0s$, the car starts accelerating the accelerator pedal value, increasing from 0 to 1 after 0.45s. The torque reaches a maximum of 205 Nm and is maintained in 2s.
- At $t = 2s$, the car starts to slow down, and braking reaches a value from 0 to 1 at time $t = 3.5s$; the torque gradually decreases to a value of -205 Nm and returns to a value of 0 at time $t = 4.66s$.

The AFPMSM motor drive system control structure applied to electric cars is shown in Figure 1.

4.2. Evaluation of Simulation Results

Two PID torque controllers are calculated with amplification parameters, PID-Isq integrals ($K_i=1.0615e+3$; $K_p=1.0744$, $K_d=1.089$). The results of searching for parameters of PID controllers using Genetic Algorithms, satisfying IAE, ITAE, and MSE quality standards, are presented in Table 1.

Table 1. Comparison of PID controllers according to design standard

Parameter	PID	GA_IAE	GA_MSE	GA_ITAE
K_p	10.2	39.996	39.1382	40
K_i	5.1	5.5288	5.5822	5.5880
K_d	1	7.5	6	8

The data in Table 1 reveals that the GA-PID controller, adjusted based on the two PID parameters in Table 1, demonstrates an MSE of 39.1382, an IAE of 39.996, and an ITAE of 40. The ITAE exhibits the highest value compared to the IAE and MSE. Consequently, this research will utilize GA_ITAE controllers to compare with the responses of traditional PID controllers.

Moreover, it is evident that the values of the PID controller’s parameters, attained by the Genetic Algorithm, significantly differ from those obtained by PID alone. This emphasizes the difficulties in fine-tuning the controller to the optimal modular standard. Although the Genetic Algorithm streamlines the optimization of three PID parameters using the MATLAB tool, its implementation is more direct.

However, the time needed for results depends on the microprocessor circuit configuration. Nevertheless, this concern has been effectively resolved through high-speed microprocessor equipment. The results of PID_ITAE’s genetic algorithm to optimize the three parameters of traditional PID torque controllers are shown in Figure 2.

The stator current responses of the torque controller are GA_ITAE_PID compared with that of the PID controller shown in Figures 3, and 4. The evaluation of the criteria of the torque control stator current response of PID and GA_ITAE_PID controllers is presented in Table 2.

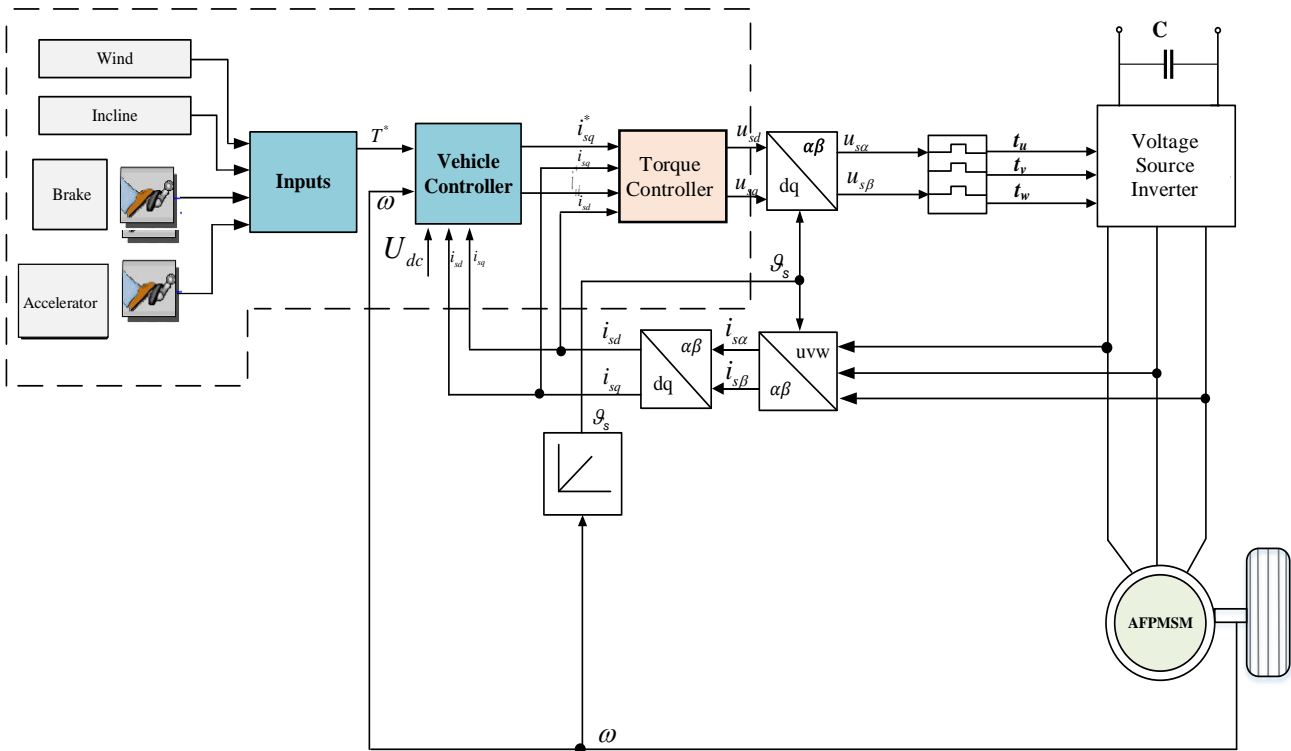


Fig. 1 The AFPMSM motor drive system control structure

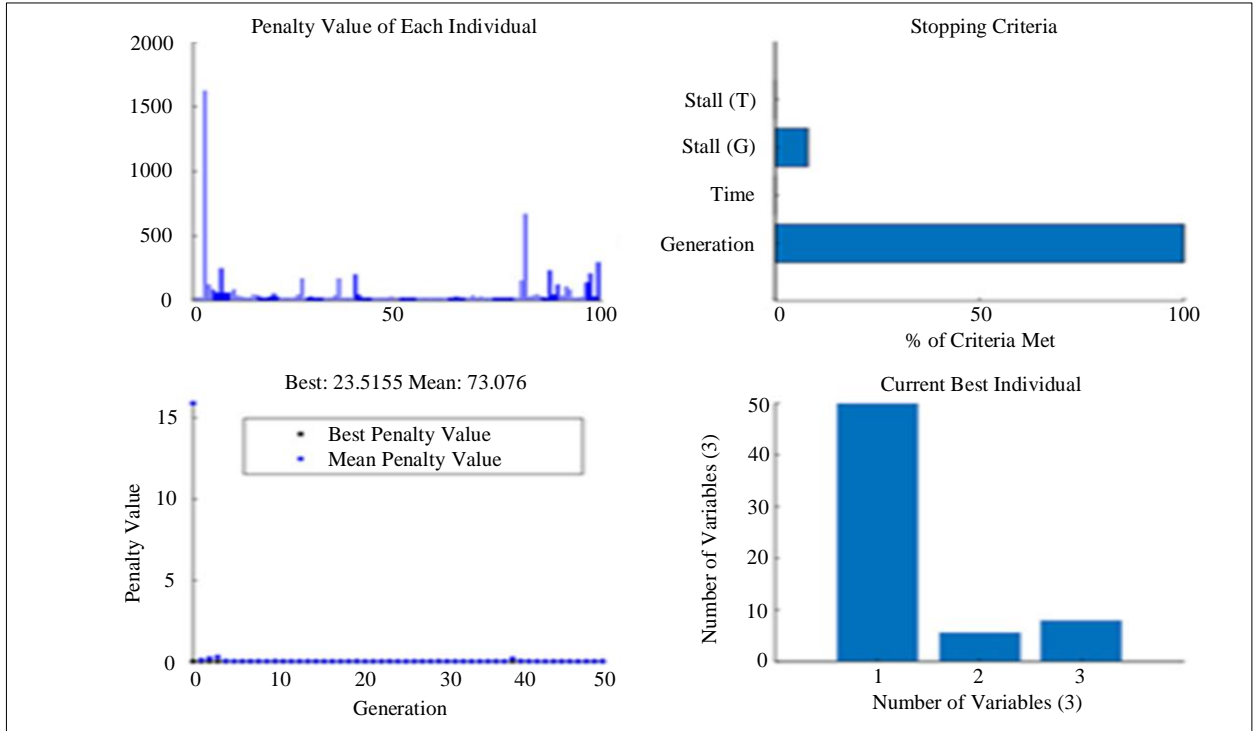
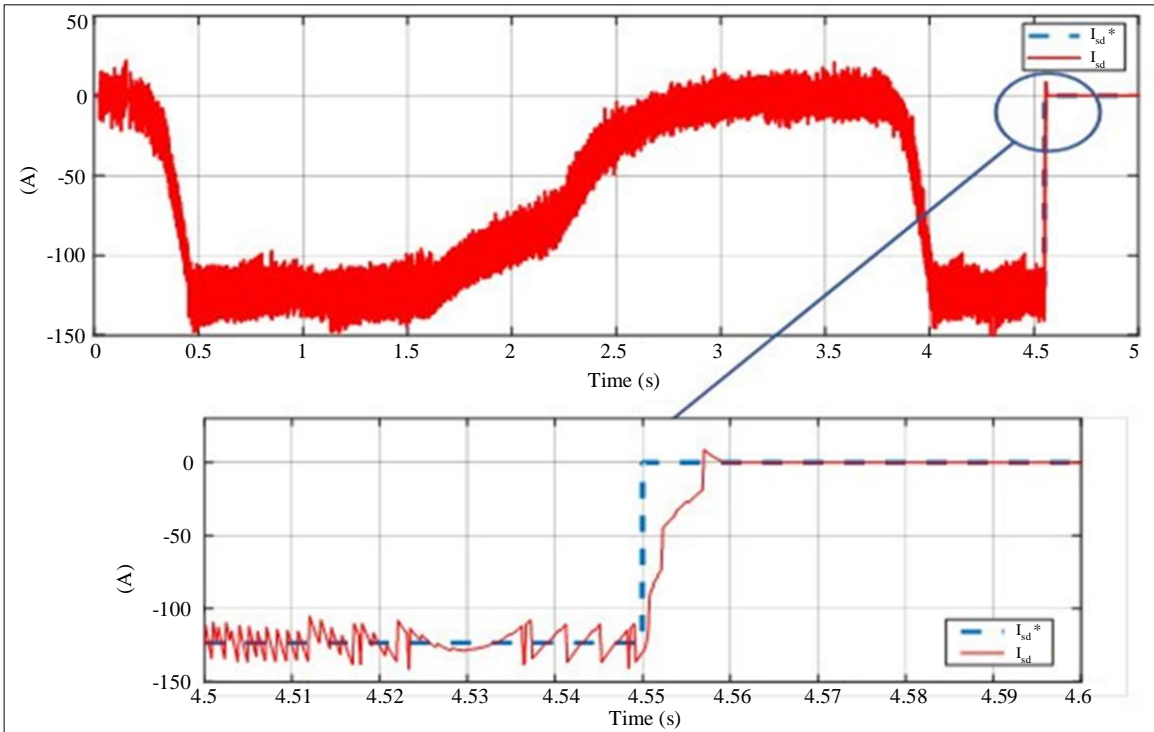
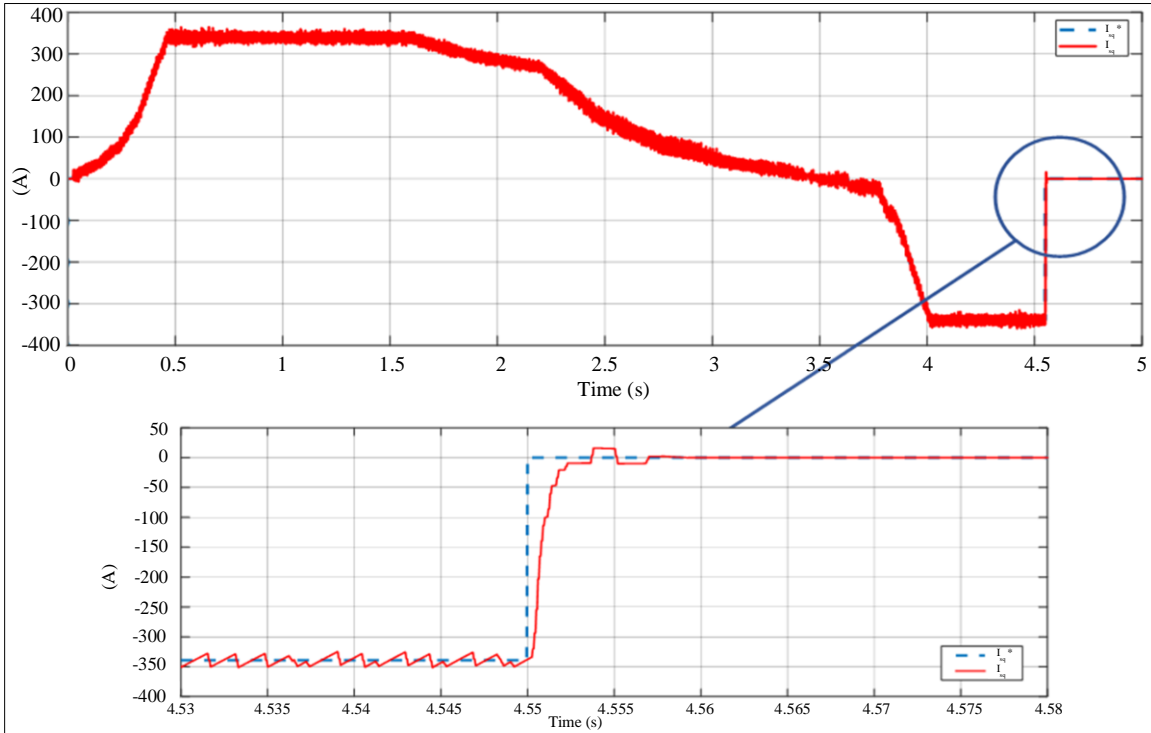
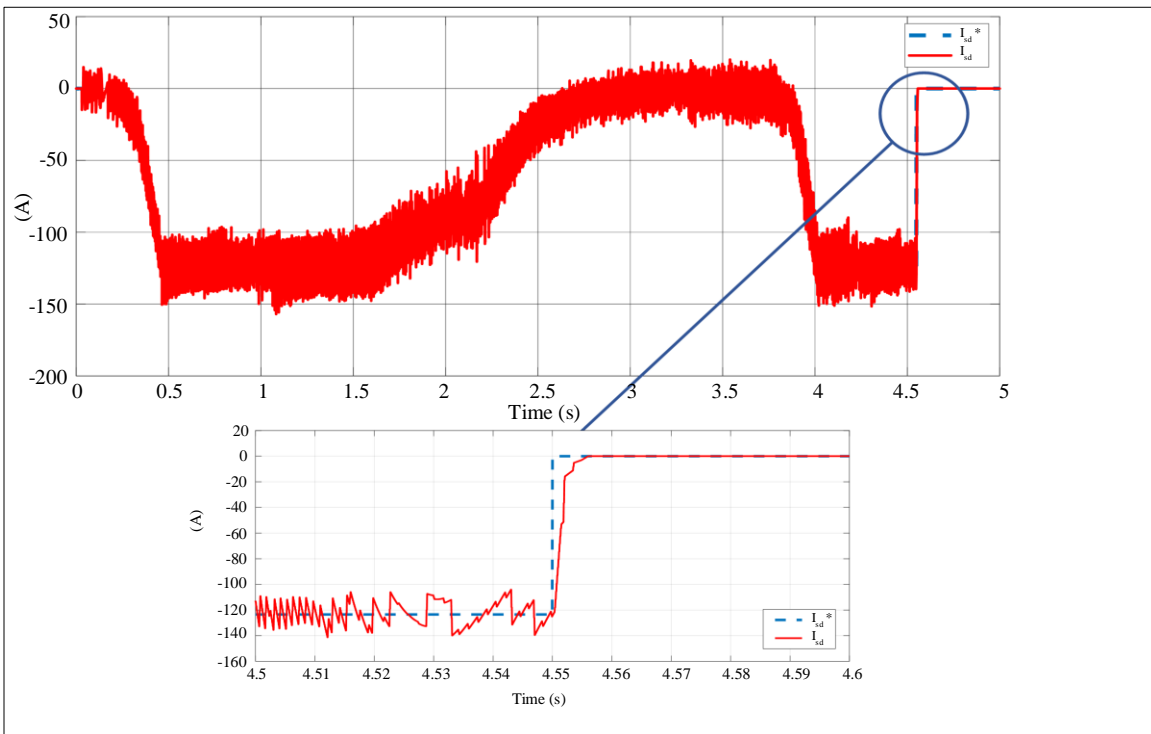


Fig. 2 Results of PID_ITAE Genetic Algorithm to optimize the three parameters of PID

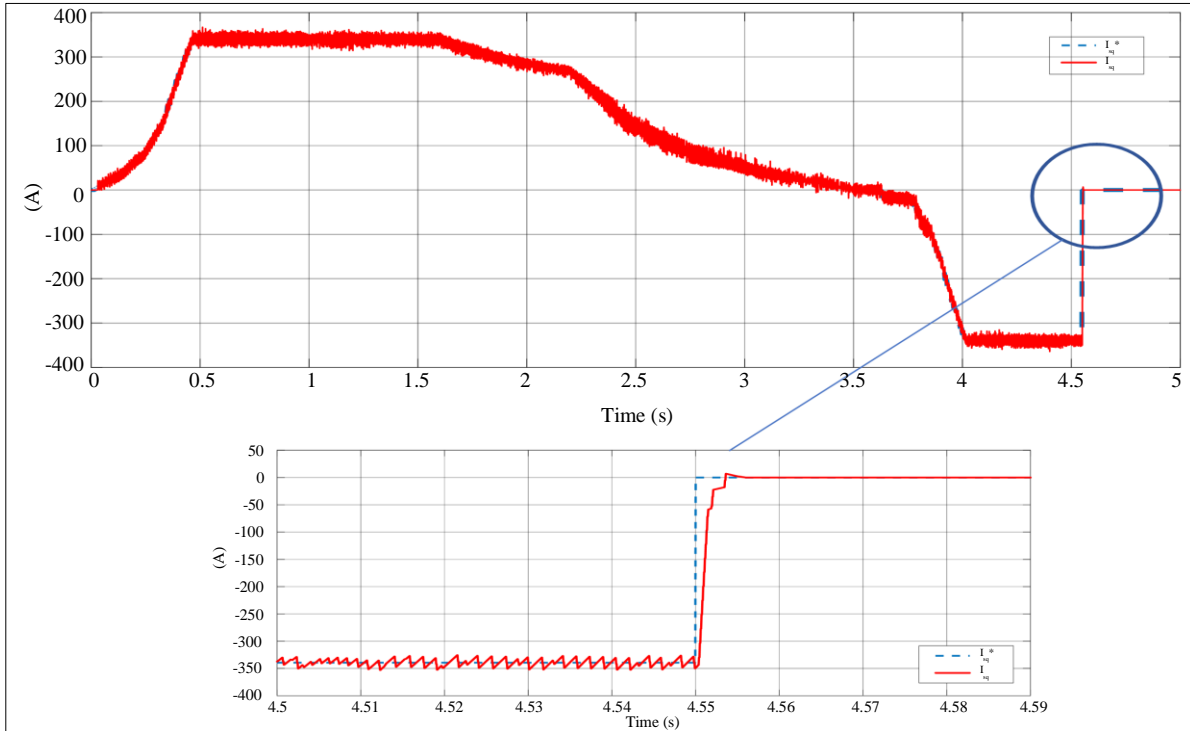




(b) Current response i_{sq}
 Fig. 3 Current stator responses of PID controller



(a) Current response i_{sd}



(b) Current response i_{sq}
Fig. 4 Current stator responses of GA_ITAE_PID controller

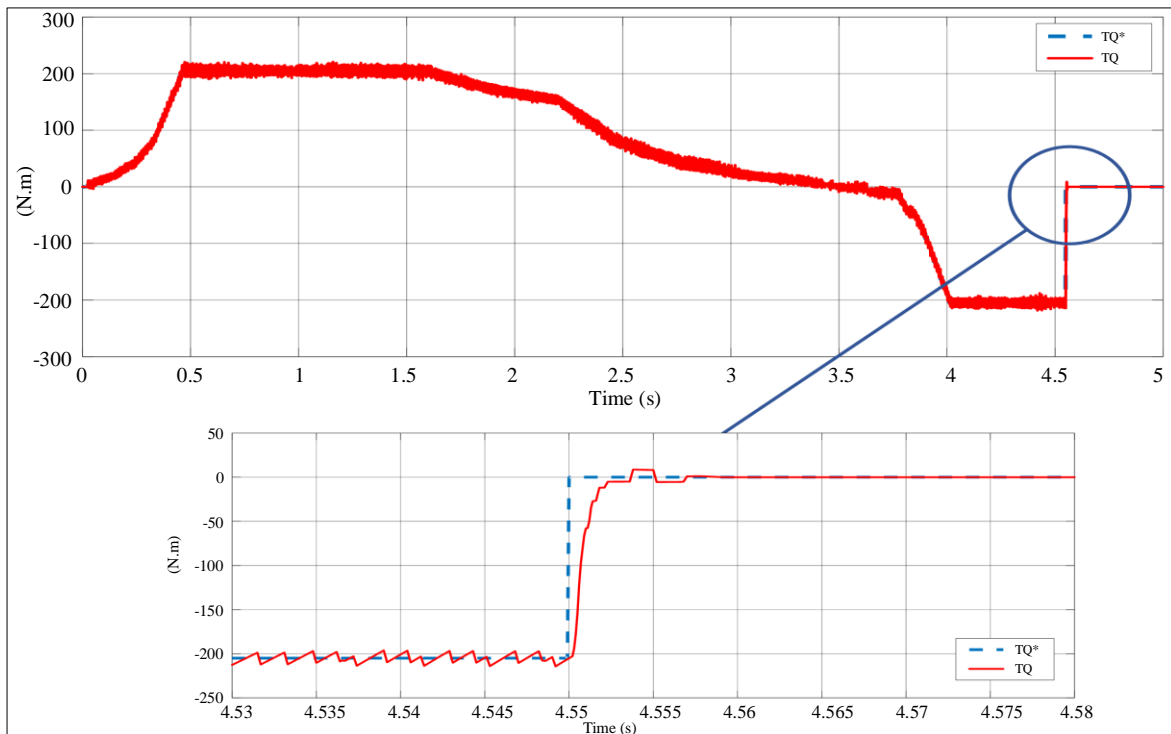


Fig. 5 The torque response of the PID controller

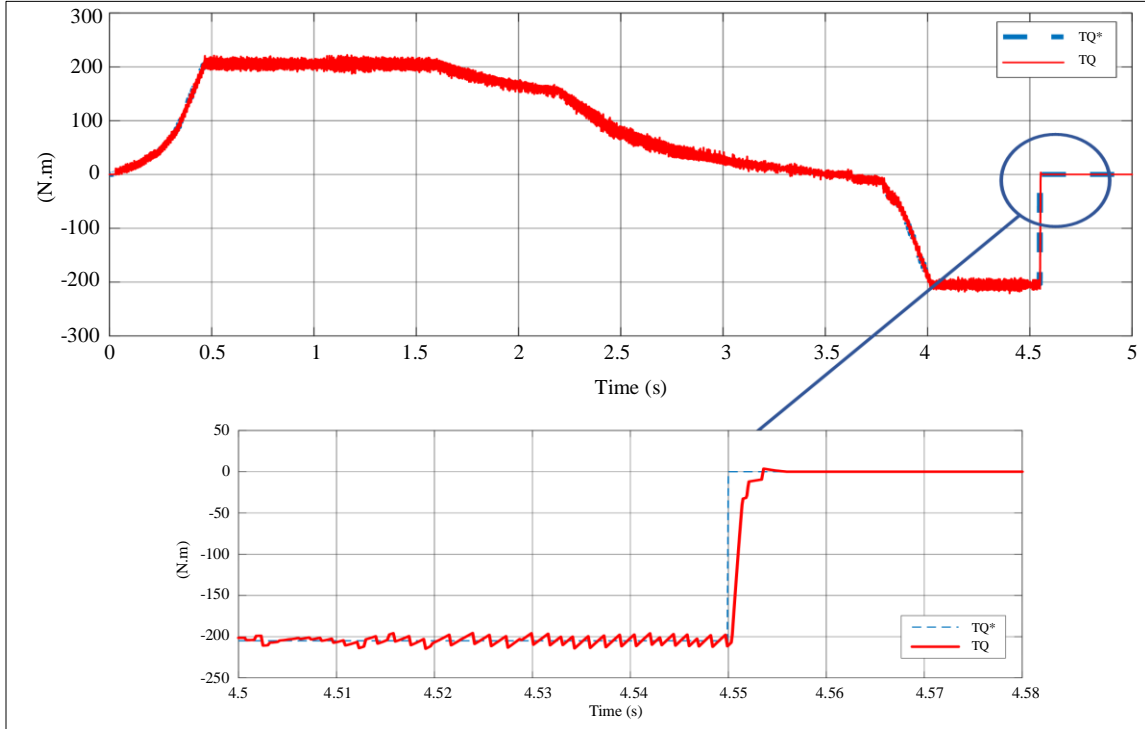


Fig. 6 The torque response of GA_ITAE_PID controller

Table 2. Stator current response assessment results of PID and GA_ITAE_PID controllers

Evaluation Parameters / Parameters	PID Controller	GA_ITAE_PID Controller
Stator Current i_{sq}		
Establishment Time	0.5(s)	0.5(s)
Too Adjustable	10%	0%

Table 3. Evaluation results of torque and speed response of PI and GA_ITAE_PID

Evaluation Criteria	PID Controller	GA_ITAE_PID Controller
Torque Circuit Beating	8%	2%

The simulation results of Figures 3, and 4 show that the stator current response of both controllers (PID and GA_ITAE_PID controllers) has a fast set time (0.5s) and is accurate in the set mode (the real signal follows the set signal). However, the GA_ITAE_PID controller gives better results than the PID controller (without too much tuning), while the PID controller with too much current regulation at the time of transition is 10%. The torque and speed responses of the torque controller are GA_ITAE_PID compared with the PI controller shown in Figures 5, and 6. The evaluation of the criteria of the torque response of PID and GA_ITAE_PID controllers is shown in Table 3. Based on the simulation results of Figures 5, and 6, it was found that the torque response of the two controllers (PID and GA_ITAE_PID controllers) is shaped like the i_{sq} current response; the actual current adheres to the set value. However, GA_ITAE_PID

controllers give a smaller circuit pulsation response (2%) than PID controllers (8%).

5. Conclusion

Research results indicate that implementing the torque controller known as GA_ITAE_PID has been proven to improve the torque response of AFPMSM in electric vehicle power trains through MATLAB simulation. Its performance matches that of a traditional PI controller. The PID and GA_ITAE_PID controllers exhibit strong performance, with the GA_ITAE_PID controller demonstrating superior overregulation and response time results. However, to validate the true effectiveness of this controller, the research team will conduct extensive research and assessment of the GA_ITAE_PID torque controller in scenarios where the motor parameters L_d and L_q vary, and the system encounters

failures. This will also consider the impact of potential future interference. This implementation will involve both offline and real-time simulation. The research team will also investigate the robustness of the GA_ITAE_PID torque controller in the presence of various disturbances, such as sudden load changes and input voltage variations. Additionally, the controller's performance will be evaluated under different operating conditions, including high-speed and low-speed operation, as well as during transient states.

This comprehensive analysis aims to validate the controller's effectiveness and reliability in real-world electric vehicle applications, ensuring its capability to handle diverse and challenging scenarios.

Acknowledgments

This research is funded by the University of Transport and Communications (UTC) under grant number T2023-DT-001 TD.

References

- [1] Xudong Zhang, Dietmar Göhlich, and Jiayuan Li, "Energy-Efficient Torque Allocation Design of Traction and Regenerative Braking for Distributed Drive Electric Vehicles," *IEEE Transactions on Vehicular Technology*, vol. 67, no. 1, pp. 285-295, 2018. [[CrossRef](#)] [[Google Scholar](#)] [[Publisher Link](#)]
- [2] Merve Yildirim, Mehmet Polat, and Hasan Kürüm, "A Survey on Comparison of Electric Motor Types and Drives Used for Electric Vehicles," *2014 16th International Power Electronics and Motion Control Conference and Exposition*, Antalya, Turkey, pp. 218-223, 2014. [[CrossRef](#)] [[Google Scholar](#)] [[Publisher Link](#)]
- [3] Tahir Aja Zarma, Ahmadu Adamu Galadima, and Maruf A. Aminu, "Reviews of Motors for Electrical Vehicles," *Journal of Scientific Research and Reports*, vol. 24, no. 6, pp. 1-6, 2019. [[CrossRef](#)] [[Google Scholar](#)] [[Publisher Link](#)]
- [4] J. Shazly, S. Wahsh, and A. Yassin, "Thermal Modeling of an AFPMSM: A Review," *Journal of Electrical Systems and Information Technology*, vol. 2, no. 1, pp. 18-26, 2015. [[CrossRef](#)] [[Google Scholar](#)] [[Publisher Link](#)]
- [5] Saber M. Saleh, and Amir Y. Hassan, "Sensorless Based SVPWM-DTC of AFPMSM for Electric Vehicles," *Scientific Reports*, vol. 12, pp. 1-12, 2022. [[CrossRef](#)] [[Google Scholar](#)] [[Publisher Link](#)]
- [6] Xavier del Toro Garcia et al., "Comparison between FOC and DTC Strategies for Permanent Magnet Synchronous Motors," *Advances in Electrical and Electronic Engineering*, vol. 5, pp. 76-81, 2011. [[Google Scholar](#)] [[Publisher Link](#)]
- [7] Shuang Wang et al., "Adaptive Robust Control System for Axial Flux Permanent Magnet Synchronous Motor of Electric Medium Bus Based on Torque Optimal Distribution Method," *Energies*, vol. 12, no. 24, pp. 1-17, 2019. [[CrossRef](#)] [[Google Scholar](#)] [[Publisher Link](#)]
- [8] Dario Crococo, Massimiliano De Agostinis, and Nicolò Vincenzi, "Structural Analysis of an Articulated Urban Bus Chassis via Finite Element Method: A Methodology Applied to A Case Study," *Journal of Mechanical Engineering*, vol. 57, no. 11, pp. 799-809, 2011. [[CrossRef](#)] [[Google Scholar](#)] [[Publisher Link](#)]
- [9] Pooja Bhatt, Hemant Mehar, and Manish Sahajwani, "Electrical Motors for Electric Vehicle - A Comparative Study," *Proceedings of Recent Advances in Interdisciplinary Trends in Engineering & Applications (RAITEA)*, pp. 1-10, 2019. [[CrossRef](#)] [[Google Scholar](#)] [[Publisher Link](#)]
- [10] Di Tan, and Chao Lu, "The Influence of the Magnetic Force Generated by the In-Wheel Motor on the Vertical and Lateral Coupling Dynamics of Electric Vehicles," *IEEE Transactions on Vehicular Technology*, vol. 65, no. 6, pp. 4655-4668, 2016. [[CrossRef](#)] [[Google Scholar](#)] [[Publisher Link](#)]
- [11] Muhammad Rafaqat Ishaque et al., "Fuzzy Logic-Based Duty Cycle Controller for the Energy Management System of Hybrid Electric Vehicles with Hybrid Energy Storage System," *Applied Sciences*, vol. 11, no. 7, pp. 1-29, 2021. [[CrossRef](#)] [[Google Scholar](#)] [[Publisher Link](#)]
- [12] Nagham S. Farhan, Abdulrahim T. Humod, and Fadhil Hasan, "Field Oriented Control of AFPMSM for Electrical Vehicle Using Adaptive Neuro-Fuzzy Inference System (ANFIS)," *Engineering and Technology Journal*, vol. 39, no. 10, pp. 1571-1582, 2021. [[CrossRef](#)] [[Google Scholar](#)] [[Publisher Link](#)]
- [13] Ramu Krishnan, *Electric Motor Drives: Modeling, Analysis, and Control*, 1st ed., Pearson Education India, 2015. [[Publisher Link](#)]
- [14] J. Yang, and V. Honavar, "Feature Subset Selection Using a Genetic Algorithm," *IEEE Intelligent Systems and their Applications*, vol. 13, no. 2, pp. 44-49, 1998. [[CrossRef](#)] [[Google Scholar](#)] [[Publisher Link](#)]
- [15] Z. Guo, and R.E. Uhrig, "Using Genetic Algorithms to Select Inputs for Neural Networks," *COGANN-92: International Workshop on Combinations of Genetic Algorithms and Neural Networks*, Baltimore, USA, pp. 223-234, 1992. [[CrossRef](#)] [[Google Scholar](#)] [[Publisher Link](#)]
- [16] Feng Tan et al., "Improving Feature Subset Selection Using a Genetic Algorithm for Microarray Gene Expression Data," *2006 IEEE International Conference on Evolutionary Computation*, Vancouver, BC, pp. 2529-2534, 2006. [[CrossRef](#)] [[Google Scholar](#)] [[Publisher Link](#)]

Appendix 1

L_{sd} and L_{sq}	The synchronous inductance on the shafts d and q.	B1	The friction coefficient.
λ_m	The flux.	J	The moment of inertia.
i_{sd}, i_{sq}	The stator current on the shafts d and q.	ω_m	The rotor speed (rad/s).
P	The number of polar pairs.	F_{aero}	Aerodynamic drag or air resistance.
T_L	The load moment.	F_{roll}	The rolling friction force of the wheel.
F	The vehicle's traction.	m_v	The total mass of the vehicle
α	The angle of inclination of the road on which the vehicle is moving.	μ	Adhesion coefficient.
F_t	The vehicle's traction.	ρ	The mass density of air.